Received June 2002
Revised April 2003
Accepted May 2003

# Mixing in a tundish and a choice of turbulence model for its prediction

Pradeep K. Jha, Rajeev Ranjan, Swasti S. Mondal and Sukanta K. Dash
*Department of Mechanical Engineering, Indian Institute of Technology, Kharagpur, India*

***Keywords*** *Turbulence, Differential equations, Modelling*

***Abstract*** *The Navier-Stokes equation and the species continuity equation have been solved numerically in a boundary fitted coordinate system comprising the geometry of a single strand bare tundish. The solution of the species continuity equation predicts the time evolution of the concentration of a tracer at the outlet of the tundish. The numerical prediction of the tracer concentration has been made with nine different turbulence models and has been compared with the experimental observation for the tundish. It has been found that the prediction from the standard k-ε model, the k-ε Chen-Kim (ck) and the standard k-ε with Yap correction (k-ε Yap), matches well with that of the experiment compared to the other turbulence models as far as gross quantities like the mean residence time and the ratio of mixed to dead volume are concerned. It has been found that the initial transient development of the tracer concentration is best predicted by the low Reynolds number Lam-Bremhorst model (LB model) and then by the k-ε RNG model, while these two models under predict the mean residence time as well as the ratio of mixed to dead volume. The Chen-Kim low Reynolds number (CK low Re) model (with and without Yap correction) as well as the constant effective viscosity model over predict the mixing parameters, i.e. the mean residence time and the ratio of mixed to dead volume. Taking the solution of the k-ε model as a starting guess for the large eddy simulation (LES), a solution for the LES could be arrived after adopting a local refinement of the cells twice so that the near wall $y^+$ could be set lower than 1. Such a refined grid gave a time-independent solution for the LES which was used to solve the species continuity equation. The LES solution slightly over predicted the mean residence time but could predict fairly well the mixed volume. However, the LES could not predict both the peaks in the tracer concentration like the k-ε, RNG and the Lam-Bremhorst model. An analysis of the tracer concentration on the bottom plane of the tundish could help to understand the presence of plug and mixed flow in it.*

## Nomenclature

| | | | |
|---|---|---|---|
| $C$ | = concentration of tracer | $t_r$ | = actual mean residence time of fluid in the vessel, equation (7) |
| $C_{av_i}$ | = average concentration of the tracer at the outlet | $u$ | = mean velocity |
| $k$ | = turbulent kinetic energy | $V$ | = volume of the tundish |
| $p$ | = pressure | $w'$ | = fluctuating velocity of $w$ component of mean velocity |
| $t$ | = time | | |

The last author, SKD, gratefully acknowledges the Alexander von Humboldt Foundation for supporting him with a high end PC on which the computations were carried out and the manuscript was prepared.

International Journal of Numerical Methods for Heat & Fluid Flow
Vol. 13 No. 8, 2003
pp. 964-996

0961-5539
DOI 10.1108/09615530310501920

$x$ = coordinate for measure of distance
$\rho$ = density of the fluid
$\mu$ = coefficient of viscosity
$\nu$ = kinematic viscosity
$\overline{u_i u_j}$ = average turbulent stress
$\varepsilon$ = rate of dissipation of turbulent kinetic energy
$\sigma_c$ = turbulent Schmidt number
$\tau$ = theoretical mean residence time, equation (7)
$\phi$ = either $k$ or $\varepsilon$

*Suffix*

$i, j, k$ = three Cartesian coordinate directions $x$, $y$ and $z$
d = dead volume
m = mixed volume
p = plug volume

## Introduction

The standard high Reynolds number $k$-$\varepsilon$ turbulence model has been widely used in industrial applications to predict the overall performance of a device. The model has been proved to be very robust and economical from the view point of computer time because of the use of standard wall functions. However, it has been observed that in recirculating flow, the prediction of near wall quantity using the $k$-$\varepsilon$ model does not compare very well with other low Reynolds number models. So, for the accurate prediction of overall quantity (the mean residence time, mixed volume and dead volume in a situation where mixing is of importance) in a device, modified forms of the standard $k$-$\varepsilon$ model have been developed in the last decade. However, such modified $k$-$\varepsilon$ models has not been used very extensively for industrial cases except its validation with simple experiments. It has been the main motivation of the present work to use the standard $k$-$\varepsilon$ model of Launder and Spalding (1972) along with its modifications, RNG (Yahkot and Orszag, 1992), Chen-Kim (CK) (Monson *et al.*, 1990) and $k$-$\varepsilon$ with Yap correction ($k$-$\varepsilon$ Yap) (Yap, 1987) to predict the mixing in a single strand tundish. The four turbulence models listed above are all of high Reynolds number form and are, of course, restricted to situations in which the Reynolds number is sufficiently high for the viscous effect to be unimportant, i.e. they can predict the flow behaviour well in the core of the tundish. However, to describe the flow close to a solid wall where the Reynolds number is not sufficiently high, low Reynolds number turbulence models with near-wall modifications have been reported to perform better (Patel *et al.*, 1984). In the present computation, we intend to use various low Reynolds number models like the Lam-Bremhorst model (LB model) (Lam and Bremharet, 1981), the Chen-Kim low Reynolds number (CK low Re) model (with and without Yap correction) and the simplest of the turbulence models the constant effective viscosity model (Phoenics Reference Guide, 1999) to obtain a relative comparison between all the turbulence models and their absolute comparison with that of the experimental investigation of Singh and Koria (1993). Finally, an attempt has been made to obtain a solution using the large eddy simulation (LES) and compare its relative accuracy with that of the experimental observation. The tundish is the last device in the sequential operation of

steelmaking where final controls can be made to improve the quality of steel and decide on its final chemistry. Hence, fluid flow and mixing in a tundish have been studied by many authors, both numerically and experimentally (Debroy and Sychterz, 1987; He and Sahai, 1987; Madias *et al.*, 1999; Szekely *et al.*, 1987; Tacke and Ludwig, 1987; Xintian *et al.*, 1992; Yeh *et al.*, 1992). However, all the mathematical models of the past have used the standard $k$-$\varepsilon$ model to compute the velocity field in the tundish and predict the tracer concentration henceforth. The effects of various turbulence models on mixing have not been reported or compared with the experimental measurements made in a tundish.

## Physical description of the problem

The geometry of the tundish is shown in Figure 1(a). The length, width and depth of the tundish are 1,000, 310 and 260 mm, respectively, with the size of the inlet and outlet as 20 mm × 20 mm. The inlet-exit distance for the tundish is 780 mm. Mixing in the tundish is studied by injecting a dye through the inlet stream for a very short time and then computing the mass concentration of the dye at the exit of the tundish as a function of time. The objective is to compute the ratio of mixed to dead volume and the mean residence time in the tundish by using various turbulence models, which are regarded as the main parameters for deciding the effective utilization of the tundish volume and hence mixing in the tundish. The response of the dye at the outlet helps to compute the mixed and the dead volume as well as the mean residence time (Jha *et al.*, 2001; Levenspiel, 1972; Szekely and Themelis, 1971). The objective is to compare the temporal variation of the concentration of the dye using all the turbulence models with that of the experimental investigation and to conclude as to which of the turbulence models predict the flow inside the tundish well.

## Mathematical formulation and assumptions

The flow field in the tundish is computed by solving the mass and momentum conservation equations in a boundary fitted coordinate system along with a set of realistic boundary conditions. The tundish boundary does not conform to a regular Cartesian system, the use of BFC was made to solve all the conservation equations. The species continuity equation is solved in a temporal manner to capture the local variation of the concentration of the dye in the tundish. The free surface of the liquid in the tundish was considered to be flat and the slag depth was considered to be insignificant. With these two assumptions the flow field was solved with the help of the following equations (in tensorial form) with all the turbulence models. The effect of natural convection is ignored in the tundish because the ratio, $\mathrm{Gr}/\mathrm{Re}^2 = 0.044\Delta T$ (Lopez-Ramirez *et al.*, 2000), where $\Delta T$, the driving force for natural convection is the temperature difference between the liquid steel at the top free surface of

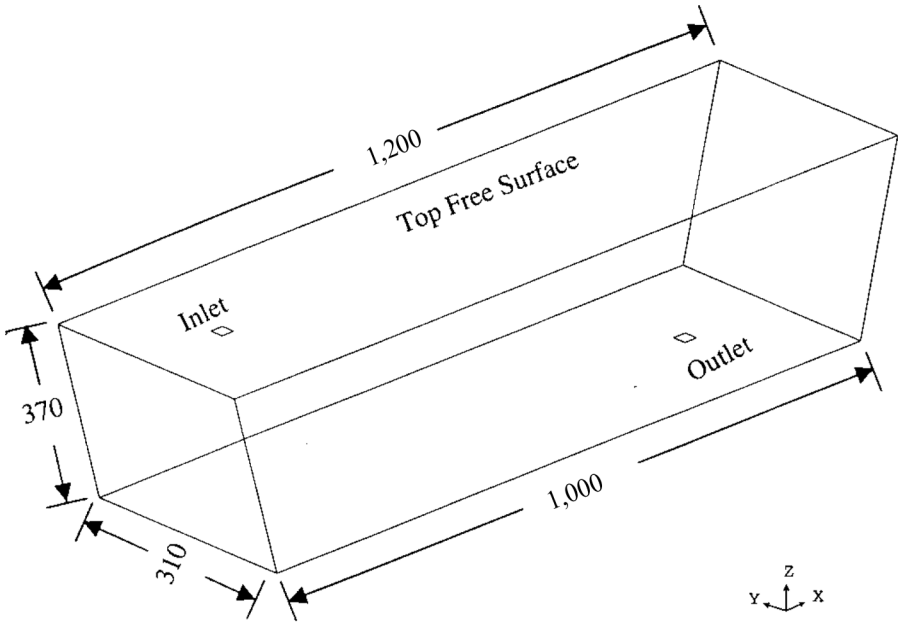


**(a)**

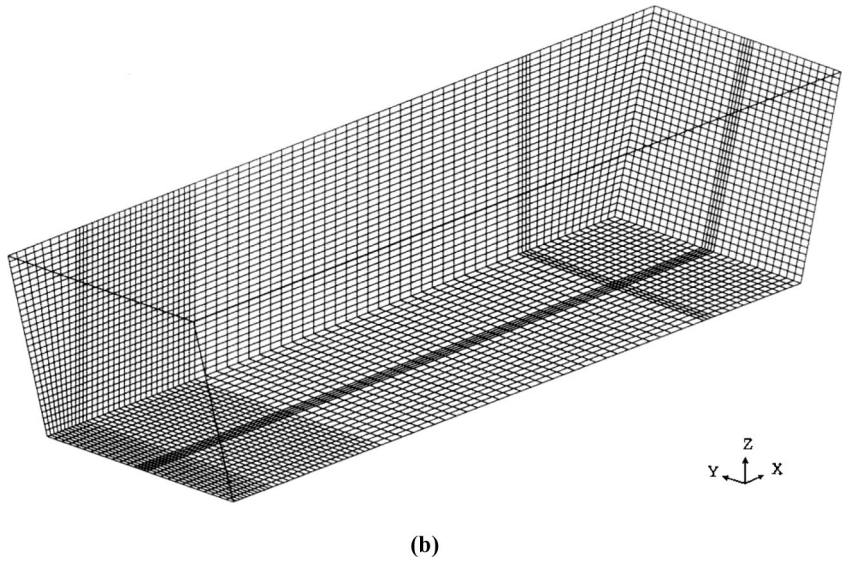


**(b)**

*(Continued)*

**Figure 1.**
(a) Geometry of the tundish used for experiment by Singh and Koria (1995) (all dimensions are in millimetre), (b) tundish of (a) with boundary fitted grid lines on the outermost surfaces, (c) tundish of (a) with boundary fitted grid lines (structured mesh) on the outermost surfaces, used for the large eddy simulation through a $k$-$\varepsilon$ starter, (d) tundish of (a) with unstructured meshes on the outermost surfaces used in the large eddy simulation (after an adaption of cells to keep $y^{+} \leq 1$)

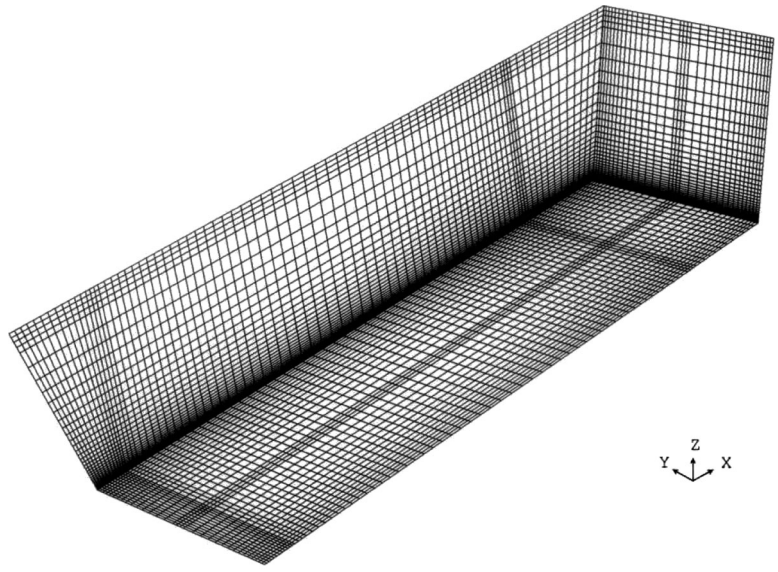


(c)

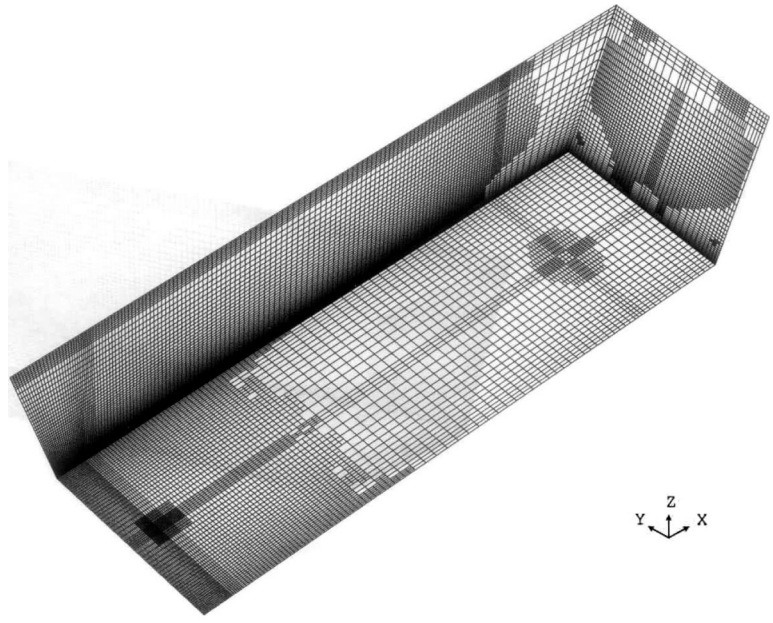


(d)

**Figure 1.**

the tundish and the bulk temperature of the liquid, which is much less than unity for all the cases that are computed here.

*Governing equations*
*Continuity*

$$\frac{\partial}{\partial x_i}(\rho U_i) = 0 \tag{1}$$

*Momentum*

$$\frac{\mathrm{D}(\rho U_i)}{\mathrm{D}t} = -\frac{\partial p}{\partial x_i} + \frac{\partial}{\partial x_j}\left[\mu\left\{\frac{\partial U_i}{\partial x_j} + \frac{\partial U_j}{\partial x_i}\right\} - \overline{\rho u_i u_j}\right] \tag{2}$$

*Turbulent kinetic energy*

$$\frac{\mathrm{D}(\rho k)}{\mathrm{D}t} = D_k + \rho P - \rho\varepsilon \tag{3}$$

*Rate of dissipation of k*

$$\frac{\mathrm{D}(\rho\varepsilon)}{Dt} = D_\varepsilon + C_1^* f_1 \rho P \frac{\varepsilon}{k} - C_2^* f_2 \frac{\rho\varepsilon^2}{k} \tag{4}$$

*Concentration*

$$\frac{\partial}{\partial t}(\rho C) + \frac{\partial}{\partial x_i}(\rho u_i C) = \frac{\partial}{\partial x_i}\left(\frac{\mu_{\mathrm{eff}}}{\sigma_{\mathrm{c}}}\frac{\partial C}{\partial x_i}\right) \tag{5}$$

where

$$\overline{u_i u_j} = \frac{2}{3}k\delta_{ij} - \nu_t\left(\frac{\partial U_i}{\partial x_j} + \frac{\partial U_j}{\partial x_i}\right)$$

$$\nu_t = C_\mu f_\mu k^2/\varepsilon, \quad \mu_{\mathrm{eff}} = \rho\nu_t + \mu$$

$$D_\phi = \frac{\partial}{\partial x_j}\left[\left(\mu + \frac{\mu_t}{\sigma_\phi}\right)\frac{\partial \phi}{\partial x_j}\right], \quad P = -\overline{u_i u_j}\frac{\partial U_i}{\partial x_j}$$

Constants used in different turbulence models are as follows.

*k-ε model*

$$C_1^* = C_1 = 1.44, \;\; C_2^* = C_2 = 1.92, \;\; \sigma_{\mathrm{c}} = 1.0$$

$$\sigma_k = 1.0, \;\; \sigma_\varepsilon = 1.3, \;\; f_1 = f_2 = f_\mu = 1, \;\; C_\mu = 0.09$$

*RNG model*

$$C_2^* = C_2 + \frac{C_\mu \eta^3 (1 - \eta/C_4)}{1 + C_5 \eta^3},$$

$\eta = Sk/\varepsilon$, $S = \sqrt{2S_{ij}S_{ij}}$ = modulus of the mean rate-of-strain tensor

$$S_{ij} = \frac{1}{2}\left(\frac{\partial U_i}{\partial x_j} + \frac{\partial U_j}{\partial x_i}\right)$$

$$C_1^* = C_1 = 1.42, \quad C_2 = 1.68, \quad C_4 = 4.38, \quad C_5 = 0.012, \quad C_\mu = 0.085$$

$$\sigma_c = 1.0, \quad \sigma_k = 1.0, \quad \sigma_\varepsilon = 1.3, \quad f_1 = f_2 = f_\mu = 1$$

*Lam-Bremhorst model*

$$f_\mu = [1 - e^{(-0.0165\,\mathrm{Re}_n)}]^2 \left(1 + \frac{20.5}{\mathrm{Re}_t}\right),$$

$$f_1 = 1 + \left(\frac{0.05}{f_\mu}\right)^3 \quad f_2 = 1 - \exp(-\mathrm{Re}_t^2), \quad \mathrm{Re}_n = \frac{\sqrt{k}Y_n}{\nu}, \quad \mathrm{Re}_t = \frac{k^2}{\nu\varepsilon}$$

$Y_n$ = distance to the nearest wall

$$C_1^* = C_1 = 1.44, \quad C_2^* = C_2 = 1.92, \quad \sigma_c = 1.0, \quad \sigma_k = 1.0, \quad \sigma_\varepsilon = 1.3,$$

$$C_\mu = 0.09$$

*Chen-Kim model*

$$C_1^* = C_1 + C_3 \frac{P}{\varepsilon}, \quad C_1 = 1.15, \quad C_3 = 0.25, \quad C_2^* = C_2 = 1.9, \quad \sigma_c = 1.0$$

$$\sigma_k = 0.75, \quad \sigma_\varepsilon = 1.3, \quad f_1 = f_2 = f_\mu = 1, \quad C_\mu = 0.09$$

*Chen-Kim low Reynolds number model*

$$f_\mu = [1 - e^{(-0.0165\,\mathrm{Re}_n)}]^2 \left(1 + \frac{20.5}{\mathrm{Re}_t}\right), \quad f_1 = 1 + (0.05/f_\mu)^3$$

$$f_2 = 1 - \exp(-\mathrm{Re}_t^2), \quad \mathrm{Re}_n = \frac{\sqrt{k}Y_n}{\nu}, \quad \mathrm{Re}_t = \frac{k^2}{\nu\varepsilon}$$

$Y_n$ = distance to the nearest wall

$$C_1^* = C_1 + C_3\frac{P}{\varepsilon},\ \ C_1 = 1.15,\ \ C_3 = 0.25,\ \ C_2^* = C_2 = 1.9,\ \ \sigma_c = 1.0$$

$$\sigma_k = 0.75,\ \ \sigma_\varepsilon = 1.3,\ \ C_\mu = 0.09$$

*k-ε with Yap correction.* An extra source term to be added in the dissipation equation (4) is

$$S_\varepsilon = \max\left\langle 0.83\rho\left(\frac{L}{L_e} - 1\right)\left(\frac{L}{L_e}\right)^2\frac{\varepsilon^2}{k}, 0\right\rangle \tag{6}$$

where $L = k^{3/2}/\varepsilon$, $L_e = 0.3C_\mu^{3/4}Y_n$, $Y_n$ = distance to the nearest wall. The constants are exactly the same as used in the *k-ε* model.

*Chen-Kim low Reynolds number model with Yap correction.* An extra source term (equation (6)) is added in the dissipation equation. The constants are exactly the same as used in the CK low Re number model.

*Constant effective viscosity model.* $k$ and $\varepsilon$ equations are not solved. $\mu$ in the momentum equation (2) is replaced by $\mu_{\text{eff}} = 200\mu_{\text{laminar}}$. The Reynolds stress term is discarded in equation (2).

*Governing equations for LES (Fluent User's Guide, 1998)*
*Continuity*

$$\frac{\partial\rho}{\partial t} + \frac{\partial\rho\bar{u}_i}{\partial x_i} = 0 \tag{7}$$

*Filtered Navier-Stokes equation*

$$\frac{\partial}{\partial t}(\rho\bar{u}_i) + \frac{\partial}{\partial x_j}(\rho\bar{u}_i\bar{u}_j) = \frac{\partial}{\partial x_j}\left(\mu\frac{\partial\bar{u}_i}{\partial x_j}\right) - \frac{\partial\bar{p}}{\partial x_i} - \frac{\partial\tau_{ij}}{\partial x_j} \tag{8}$$

where $\tau_{ij}$ is the subgrid-scale stress defined by

$$\tau_{ij} = \rho\overline{u_i u_j} - \rho\bar{u}_i\bar{u}_j$$

(notice the similarity with Reynolds stress as well as the difference from it, $\rho\bar{u}_i\bar{u}_j$ being the extra term subtracted from the Reynolds stress). The majority of subgrid-scale models are eddy viscosity models of the following form

$$\tau_{ij} - \frac{1}{3}\tau_{kk}\delta_{ij} = -2\mu_t\bar{S}_{ij}$$

where $\mu_t$ is the subgrid-scale turbulent viscosity and $\bar{S}_{ij}$ is the rate of strain tensor for the resolved scale defined by,

$$\bar{S}_{ij} = \frac{1}{2}\left(\frac{\partial \bar{u}_i}{\partial x_j} + \frac{\partial \bar{u}_j}{\partial x_i}\right)$$

*RNG based subgrid scale model.* Effective subgrid viscosity $\mu_{\text{eff}} = \mu + \mu_t$ is given by,

$$\mu_{\text{eff}} = \mu\left[1 + H\left(\frac{\mu_s^2 \mu_{\text{eff}}}{\mu^3} - C\right)\right]^{1/3}$$

where,

$$\mu_s = (C_{\text{rng}} V^{1/3})^2 \sqrt{2\bar{S}_{ij}\bar{S}_{ij}}$$

and $H(x)$ is the Heaviside function (ramp function):

$$H(x) = \begin{cases} x, & x > 0 \\ 0, & x \leq 0 \end{cases}$$

and $V$ is the volume of the computational cell, and

$$C_{\text{rng}} = 0.157$$

$$C = 100$$

In highly turbulent regions of the flow ($\mu_t \gg \mu$), $\mu_{\text{eff}} \cong \mu_s$, and the RNG-based subgrid-scale model reduces to the Smagorinsky-Lilly model with a different model constant. In low Reynolds number regions of the flow, the argument of the ramp function becomes negative and the effective viscosity recovers molecular viscosity. This enables the RNG-based subgrid-scale eddy viscosity to model the low Reynolds number effects encountered in transitional flows and near-wall regions.

## Computation of mixed and dead volume (Jha *et al.*, 2001; Levelspiel, 1972; Szekely and Themelis, 1971)

$$\text{Theoretical residence time } \tau = \text{volume of tundish}/(\text{volumetric flow rate}) \tag{9}$$

Actual residence time

$$t_r = \frac{\sum C_{\text{av}_i} t_i}{\sum C_{\text{av}_i}}, \quad i = 1 \text{ (for single outlet)} \tag{10}$$

In equation (10), the integration is carried over a time span of $2\tau$ with an equal interval of time step.

$$\text{Average breakthrough time, } t_p = \text{First appearance of tracer at the exit} \tag{11}$$

The dead volume is computed from equation (12) after computing the theoretical and actual mean residence time from equations (9) and (10), respectively. The mixed volume is computed from equation (14) after the dead and plug volumes are computed.

$$\text{Fraction of dead volume, } V_d/V = 1 - t_r/\tau \tag{12}$$

$$\text{Fraction of plug volume, } V_p/V = t_p/\tau \tag{13}$$

$$\text{Fraction of mixed volume, } V_m/V = 1 - V_p/V - V_d/V \tag{14}$$

## Boundary conditions

The walls were set to a no slip condition and the turbulent quantities were set from a log law wall function for the $k$-$\varepsilon$, $k$-$\varepsilon$ RNG, $k$-$\varepsilon$ CK and $k$-$\varepsilon$ with Yap correction models. The following "logarithmic law of the wall" (Ferziger and Peric, 1999) was utilized to compute the value of $k$ ($k_p$) and $\varepsilon$ ($\varepsilon_p$) at the first cell in contact with the wall by considering the production and dissipation of turbulent quantities to be in local equilibrium near the wall.

$$\frac{\rho u_p k_p^{1/2} C_\mu^{1/4}}{\tau_w} = \frac{1}{\kappa} \ln(Ez^+),$$

where

$$z^+ = \frac{z_p k_p^{1/2} C_\mu^{1/4}}{\nu}, \quad E = 8.6$$

and

$$\kappa = 0.41, \quad \varepsilon_p = \frac{C_\mu^{3/4} k_p^{3/2}}{\kappa z_p}$$

It can be noticed from the above equation that the first node distance from the wall, $z_p$ influences the near wall turbulent quantities. The influence of $z_p$ on mixing parameters ($V_m/V$, $V_p/V$ and $V_d/V$) is studied in the present computation in order to arrive at a suitable grid distribution near the wall which can predict more accurate results for mixing.

For the low Reynolds number turbulence models, $k = 0$ and the normal gradient of $\varepsilon$ to the wall was set to 0. At the inlet, the velocity of the incoming jet was set to a prescribed value of 0.3875 m/s (in accordance with the

experiment) with a turbulent intensity of 2 per cent. The intensity of turbulence is defined here to be

$$I = \sqrt{\frac{\overline{w'}^2}{w_{\text{inlet}}}},$$

from which the value of $k$ at the inlet can be prescribed as $k = 0.5(Iw_{\text{inlet}})^2$. The value of $\varepsilon$ at the inlet is computed from the relation

$$\varepsilon_{\text{inlet}} = \frac{C_\mu^{3/4} k_{\text{inlet}}^{3/2}}{0.1H},$$

where $H$ is the hydraulic radius of the inlet pipe (Launder and Spalding, 1972). There exists symmetry on an $x$-$z$ plane (a vertical plane passing through the inlet and outlet), where symmetry conditions for all the variables have been used. However, the grids and the contour plots are shown in full for a better visualization.

For the LES the inlet velocity condition was prescribed at the inlet with a turbulence intensity of 2 per cent and all other boundary conditions were treated exactly like the laminar flow solution. Here it must be noticed that $k$ or $\varepsilon$ does not appear in the LES solution, so their prescription as a boundary condition is not required at all. The filtered quantity like, $\bar{u}_i$, $\bar{u}_j$ are exactly treated like the laminar variables and are prescribed to be zero at the walls. At the top free surface, at the vertical symmetry plane passing through the inlet and outlet (i.e. the $x$-$z$ plane when half geometry is considered) and at the outlet they are given a zero gradient condition for the LES.

The top surface of the tundish was taken to be a free surface where a zero shear stress condition was applied according to Illegbusi and Szekely (1989), Szekely *et al.* (1987) and Tacke and Ludwig (1987). The bottom of the tundish was treated like a wall where no slip conditions were used for the velocity. At the outlet a fixed pressure of 0 Pa (relative to the ambient) was applied. The wall of the tundish was considered to be impervious to the dye, so a zero gradient condition for the dye was used on the walls. At the outlet and at the free surface also zero gradient conditions for the dye were used (Illegbusi and Szekely, 1988, 1989). At the inlet the concentration of the dye was kept at 1 from 1 to 5 s after which the concentration was kept at zero. Five seconds is normally very short compared to the mean residence time of the tundish so the influx of the dye during its travel is not likely to change the local velocity field as the mass influx of the dye is also very small Szekely and Themelis, 1971).

## Method of solution

The set of partial differential equations (1)-(5) was solved numerically with the help of the above boundary conditions in a finite volume technique using the

educational version of the CFD software Phoenics and the differential equations (7) and (8) were also solved in a finite volume method by adopting a unstructured grid due to local refinement by the educational version of the CFD software Fluent. The partial differential equations were integrated over a control volume to find out the fluxes (of mass and momentum as well as that of the dye) through all the faces, and the flux balance is made over all the control volumes, which yield a set of linear algebraic equations. The set of algebraic equations is solved by the tridiagonal matrix (TDM) method for momentum and by a whole field solver, taking one from the family of conjugate gradients for the pressure correction equation. The species continuity equation is solved at each and every time step using the TDM matrix method once the steady state solution for the momentum equations is obtained. The solutions are said to have converged when the whole field normalized residuals for each of the velocity components and mass fall below unity. A false time step relaxation of 0.5 was used for all the variables for faster convergence.

*High Reynolds number models*

Control volumes (CV) of $76 \times 14 \times 30$ ($X \times Y \times Z$) were used for the computation of the single strand bare tundish for the high Reynolds number models taking the vertical plane passing through the inlet and outlet to be a plane of symmetry (grid shown in Figure 1(b) for the entire tundish for better visualization). Grid refinement (Figure 1(b)) is made closer to the point of impingement to avoid any artificial diffusion coming out of the hybrid scheme. More on this will be discussed later in the "Results and discussions" section. By changing the control volumes to $126 \times 28 \times 60$, it was observed that the changes in the mixed and dead volumes were less than 0.1 per cent. Hybrid differencing scheme for the convective fluxes and central differencing for the diffusive fluxes were used at the cell faces for all high and low Re number models. Also a non-linear higher order smooth scheme (HOS) called "SMART" was used for the $k$-$\varepsilon$ and the RNG model to assess the extent of artificial diffusion coming out of the discretization. The higher order scheme was used only for the convective fluxes in the solution of the momentum and species continuity equation while hybrid scheme was used to compute the convective fluxes for the solution of the turbulent quantities. It was observed that with the use of SMART scheme, grid independent solution could be arrived at relatively coarse grids ($41 \times 8 \times 15$) for the $k$-$\varepsilon$ and the RNG model (see Figure 2(d) and (e) for a comparison of the grid independent solution). However, the non-linear higher order scheme, "SMART" did not give very accurate solution compared with the experiment.

*Low Reynolds number models*

For the low Reynolds number models control volumes of $90 \times 20 \times 41$ ($X \times Y \times Z$) were used which could yield a $z^+$ value of nearly 1 or

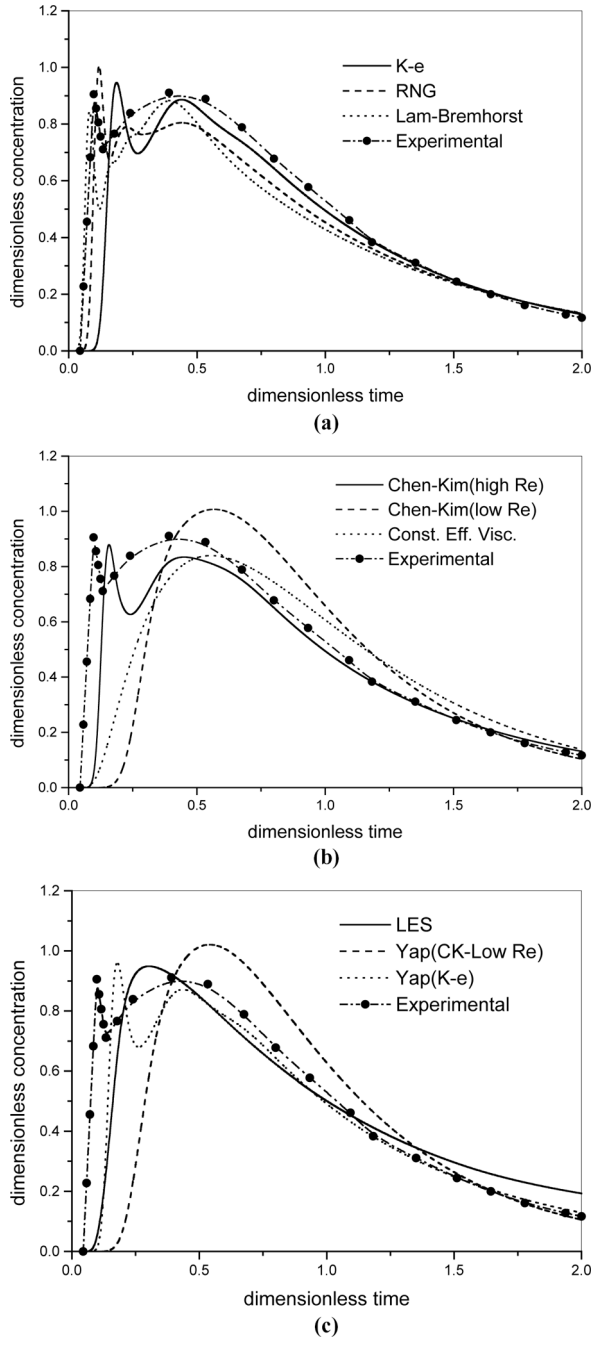


**Figure 2.**
(a-c) Temporal variation of tracer concentration at the outlet of a single strand tundish: a comparision between experiment and various turbulence models, (d, e): temporal variation of tracer concentration at the outlet of a single strand tundish: a comparative analysis between lower and higher order differencing scheme and a test for grid independency

*(Continued)*

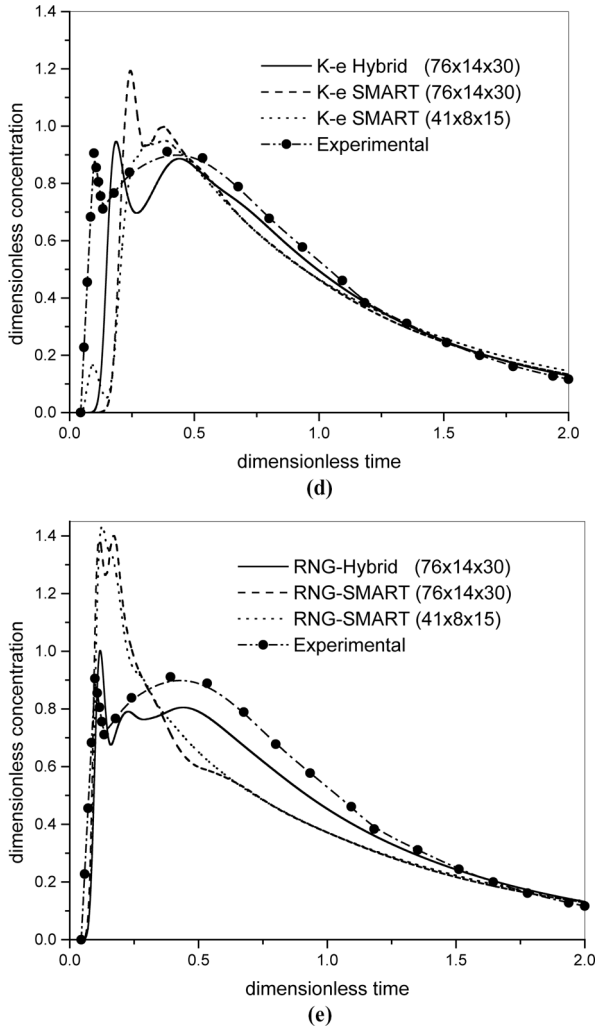


**Figure 2.**

somewhere less than 1 near the tundish wall. Increasing the CVs to $(150 \times 34 \times 70)$ no perceptible difference in the mean residence time and mixed volume were observed. Hybrid differencing scheme was used for the low Re number model to evaluate the convective fluxes in the momentum as well as in the species continuity equation. The use of higher order scheme, "SMART" or even "QUICK" did not produce a converged solution (for the above sets of grids) for the low Re number models for which they could not be reported here.

*Solution of LES*

For the solution of LES, a structured grid of $80 \times 34 \times 37$ was created (Figure 1(c)) (for simulation in the entire tundish) in which first a solution of the velocity field was obtained by employing the $k$-$\varepsilon$ model. Also the same grid structure of Figure 1(c) was employed to arrive at a velocity field in half of the tundish by employing the symmetry condition at the plane passing through the inlet and the outlet. This solution of the velocity field was treated as an initial guess for the LES solution in both the cases (half and full geometry). The LES was made to run with a time step of 0.001 s for about 2,000 time steps by which time the fluctuations in the outlet velocity could die out severely. In the LES solution the convective variables were approximated by the QUICK scheme and the pressure correction routine was solved by the PISO algorithm. The $y^+$ was computed in the solution domain and the cells were refined in order to produce a value of $y^+$ nearly 1 near the walls. Such an adopted mesh is shown in Figure 1(d) (158,756 cells in total) in which the final computation for LES was carried out. It is interesting to note that the region close to the point of jet impingement has been adapted to finer cells automatically (Figure 1(d)). The top free surface is deliberately given finer cells in order to capture velocity variations if any created due to the rising plume from the jet impingement. The final computation for LES was carried out on the mesh shown in Figure 1(d) (shown with full geometry for a better visualization of the grid arrangement) and a time independent solution could be arrived after a run of 16 s with a time step of 0.001 s for each step. After the computation of the velocity field the solution for the species continuity equation was initiated in a transient manner. It has to be noted here that both the solutions, half and full geometry, gave identical solutions in the case of the LES.

From the temporal variation of concentration the actual mean residence time and all other times were found out by simple integration (equation (10)) after which the ratio of mixed to dead volume could be found out. For the computation, the density of the working fluid (water) was taken to be $998.3\,\mathrm{kg/m^3}$ all through the volume and the kinematic viscosity (Mazumdar and Guthrie, 1999) to be $1.0 \times 10^{-6}\,\mathrm{m^2/s}$.

## Results and discussions

The flow field in the tundish was obtained by solving the Navier-Stokes equations numerically and then the tracer dispersion was computed by injecting some dye into the inlet. From the tracer dispersion curve the mixed volume and the dead volume were computed as per equations (12), (13) and (14). The analysis of mixing was done with respect to the ratio of mixed to dead volume and the mean residence time of the tundish by using many different turbulence models. The mixed and the dead volumes are direct indices of mixing in a tundish. If the mixed volume is large that means more of the tundish volume is utilized in mixing the fluid. In a similar way, it can be said

that if the dead volume is low then most of the volume of the tundish is utilized by the fluid for mixing. So a ratio of the mixed to dead volume (Singh and Koria, 1995) and the mean residence time are better parameters to describe the mixing in a tundish. We will discuss the temporal variation of tracer concentration and then the ratio of mixed to dead volume ($V_m/V_d$) and the mean residence time for all the turbulence models to compare them with the experimentally obtained values.

*RTD analysis*

Singh and Koria (1993) have done the experiment for a single outlet tundish in which they have measured the tracer concentration with time at the outlet. The geometry of the tundish is shown in Figure 1(a) and the computational cells used in the present computation are shown in Figure 1(b) for the high Re number models only. In the experiment, the bath height was kept at 260 mm and accordingly the same height was used for the computation where the free surface boundary condition was applied. Figure 2(a)-(e) shows the temporal variation of the tracer concentration (dimensionless concentration) with non-dimensional time and its comparison with all the turbulence models. It can be seen from the figures that the tracer concentration has two peaks in the experiment (one at $t = 0.15$ and the other at $t = 0.42$) and all the high Reynolds number models are able to predict both the peaks but they have their own delays in time while predicting them whereas all the low Reynolds number turbulence models except the LB model shows only one peak including the prediction of LES.

When the tracer is first added at the inlet it moves with the flow field towards the outlet due to the steady velocity field present in the tundish. It takes little time to reach the outlet and that can be seen clearly in Figure 2(a) when the concentration just starts to rise from a value of zero. The concentration at the outlet then increases with time due to a continuous feed of tracer material from the near wall region of the tundish. A sharp increase in the tracer concentration shows that mixing has not taken place in the tundish, because the tracer that has been added has just found its way to the outlet (by the side of the wall or through the center line) for which there is a sudden jump in the concentration at the outlet. If there were mixing then the change in the concentration at the outlet could be gradual, which is seen to be happening at a later time ($t > 0.5$). However after the initial peak, the tracer concentration falls suddenly and then gradually increases to another peak after which it slowly decreases with time. This happens because after the sudden release of tracer material at the outlet (arriving from the near wall) there is no tracer present around the outlet for which the concentration suddenly falls. However, after a while the fluid brings a continuous stream of tracer through the center line of the tundish which is fed to the outlet for which the concentration again increases and attains a peak value. This time the tracer concentration does not

increase as suddenly as it does the first time. This effect is captured well by the RNG, the LB and the CK high Re number model where there is a gradual increase of tracer concentration to the second peak. After the second peak the tracer slowly goes out of the system for which the concentration slowly falls with time and after about two times the mean residence time, the concentration falls to nearly zero. So it can be found from this experimental observation that mixing has really taken place after a non-dimensional time of 0.2 from when the rise in tracer concentration has become gradual as well as its fall.

It should be observed in Figure 2(b) that the CK low Re number model and the constant effective viscosity model show a gradual rise and fall of the tracer concentration with time and both the models show only one peak in the concentration curve. The CK low Re number model employs exactly the same near wall modifications like the LB model but the second term in the right of equation (4) differs in both the models. The CK low Re model employs one more extra term ($C_3P/\varepsilon$) in the dissipation of the production of turbulent kinetic energy in the dissipation equation. This helps to dampen dissipation and hence the overall turbulent kinetic energy near the wall as well as in the core of the tundish remains high causing more of turbulent mixing in the entire tundish. So the tracer concentration rises gradually like the constant effective viscosity model where the effect of turbulence is artificially put to be higher by making the effective viscosity to be 200 times the laminar viscosity. The CK high Re number model does not use the near wall modifications of the LB model so the dissipation remains high near the wall which produces lower values of turbulent kinetic energy similar to the $k$-$\varepsilon$ model. Hence both the $k$-$\varepsilon$ and its CK modification behave almost the same way as far as the tracer dispersion is concerned.

Figure 2(c) shows the effect of Yap correction on the standard $k$-$\varepsilon$ high Re number model as well as for the CK Low Re number model. The use of the Yap correction helps to decrease dissipation which produces lower values of $\varepsilon$ thus producing higher values of turbulent kinetic energy near the wall. So in general the performance of the high Re number turbulence as well as that of the low Re numbers turbulence model becomes better. This can be seen in Figure 2(c) for the standard $k$-$\varepsilon$ as well as for the CK low Re number model where both the models predict little better when compared with the experiment. But the effect of the Yap correction does not seem to be significant for the present numerical simulation.

It can be seen that all the high Reynolds number models show double peak as the low Reynolds number models (including the LES) except the LB model which shows a single peak. Also the models which have shown a single peak, the first appearance of tracer is delayed too much in those models due to the use of an overall higher field values of $k$ which aids diffusional mixing causing a delay in the appearance of the tracer at the outlet. However, the LES does not

show a large delay in the first appearance of the tracer and it also predicts the peak value of the concentration very well which compares with the experimental observation. The initial appearance of tracer has best been predicted by LB model and then by RNG model. However, in these two models which show a better match in the initial period of tracer movement, the matching does not seem to be better in the later part of the curve. The temporal value of the concentration for these two turbulence models are less than that of the experiment after a dimensionless time ($t$) of 0.5. Hence these two models show an under predicted value of mean residence time as well as ratio of mixed to dead volume than the experimentally predicted one. For high Reynolds number models except the RNG model, there is some initial delay in predicting the first appearance of the tracer at the outlet but the matching seems to be well after a dimensionless time of 0.5.

In order to get a better prediction of the mean residence time and the ratio of the mixed to dead volume it is important that the tracer concentration should match well with the experimental observation after a time of 0.5 because the computation of these quantities depends on the first area moment of the concentration curve about the concentration axis. So an initial mismatch of tracer concentration with time does not contribute much to the computation of mean residence time as well as to the ratio of mixed to dead volume where as the contribution from a later time matter much because the computation of area moment (equation (10)) about the concentration axis directly multiplies the time. Due to this reason, the $k$-$\varepsilon$ model shows a better match of properties (like the mean residence time and the ratio of the mixed to dead volume) compared to the RNG and the LB model although the initial prediction of the tracer concentration is not that good compared to the RNG and the LB model. In the case of low Reynolds number models except the LB model, the initial appearance of the tracer is delayed considerably as well as the matching in the later part of the curve is also not good in the sense that the temporal value of the concentration for these models are higher than that of the experimentally obtained one. This results in the over prediction of mean residence time as well as ratio of mixed to dead volume. For constant effective viscosity model, the initial prediction of tracer concentration is same as that of high Reynolds number models but the matching in the later part is not good and it over predicts the mixing parameter.

Figure 2(d) and (e) show the temporal variation of concentration at the outlet with the use of higher order differencing schemes (HOS) for the convective variables. The SMART scheme is used for the $k$-$\varepsilon$ and the RNG model. The convective variable $\phi$ at the cell face (f) has been approximated in the following manner in the SMART scheme.

$$\phi_f = \phi_c + 0.5B(r)(\phi_c - \phi_u)$$

where $B(r)$ is termed a limiter function, and the gradient ratio $r$ is defined as

$$r = \frac{\phi_d - \phi_c}{\phi_c - \phi_u}$$

$$B(r) = \max\left[0, \min\left(2r, \frac{3}{4}r + \frac{1}{4}, 4\right)\right]$$

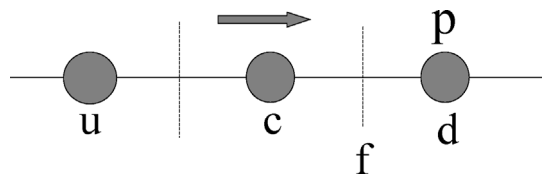


It can be observed from the figure that the HOS scheme is able to predict both the peaks in the concentration for the RNG model and with a grid size of $76 \times 14 \times 30$ for the $k$-$\varepsilon$ model almost where the hybrid scheme predicts the second peak. With a lesser number of cells the $k$-$\varepsilon$ model with a HOS scheme predicts the first peak very exactly at the time where the experiment shows its first peak. However, the peak concentration (first peak) predicted from the $k$-$\varepsilon$ (HOS) is much lower compared to the peak concentration value of the experiment. In the $k$-$\varepsilon$ as well as in the RNG model it can be observed that almost a grid independent solution could be achieved at less number of grids which was not so for the hybrid differencing scheme. The hybrid scheme required larger number of grids in order to produce a grid independent solution. However, the use of HOS could not produce very accurate results compared with the experimental observation. The peak concentration values predicted with the HOS scheme did not match very well with the experimental observation.

Turbulence is generated in the vicinity of the jet impingement and slowly the flow goes over a transition and becomes laminar in the core of the tundish and then again towards the outlet it becomes turbulent. There are transitions in the flow and simple turbulent models like $k$-$\varepsilon$ and the RNG cannot adopt itself to predict this type of flow very well. Whereas the LB model to some extent does it by incorporating wall dissipation to the eddy viscosity coefficients. The LES is believed to predict a transition from turbulence to laminar but the flow predicted by the LES seems to be thoroughly mixed, although it shows the presence of plug flow in the tundish. The reason for this will be discussed later.

It was suspected that the near wall turbulent quantities computed from the logarithmic wall function could be producing higher values of $k$ for the $k$-$\varepsilon$ turbulence model for which the first appearance of tracer at the outlet is delayed compared with the experimental observation. So in order to examine

the effect of the "log law wall function" on mixing, the first node distance from the bottom wall ($z_p$) was changed according to the suggestion given by Chakraborty and Sahai (1991). Figure 3 shows the effect of near wall node on the temporal variation of tracer concentration at the exit of a single strand tundish (Singh and Koria, 1991). The near wall node distance, $z_p$ was varied from 4.39 (maximum $z^+ = 18$) to 13 mm (maximum $z^+ = 40$) in the $k$-$\varepsilon$ turbulence model but the mean residence time was changed only from 444.51 to 445.7 s, respectively. It can be seen from Figure 3 that the first peak in the concentration curve is predicted little higher when $z_p$ is 4.39 mm and subsequently with the increase of $z_p$ to 13 mm the peak decreases. Both the peaks are predicted very near to the experimental observation when $z_p$ has a value of 8.67 mm (maximum $z^+ = 30$). But the initial delay in appearance of the tracer is nearly the same for all the cases of $z_p$ studied here. From Table I, a comparison of the various mixing parameters can be read for different turbulence models. It can be concluded that the grid distribution, with a near wall node located at 8.67 mm is more suitable for predicting the experimental observation.

*Analysis of Iso-concentration lines*

Figures 4-9(a)-(c) show the iso-concentration lines at different times at the bottom of the tundish for four different turbulence models, i.e. the $k$-$\varepsilon$, the RNG, the LB and the LES. The iso-concentration lines at time $t = 10$ s are shown in Figure 4(a)-(c) for three models while in Figure 9(a) the concentration distribution can be seen from the LES. When the liquid jet hits the bottom of the tundish, it just spreads over it and so also the tracer along with it because it simply gets convected by the stream. So the concentration is seen to be highest at this point (a point just below the inlet) for all the four turbulence models. From this point the tracer is convected as well as diffused in all other direction. The flow remains to be wall bounded for all the four turbulence models for which the concentration plots at the bottom of the tundish, is shown. When the

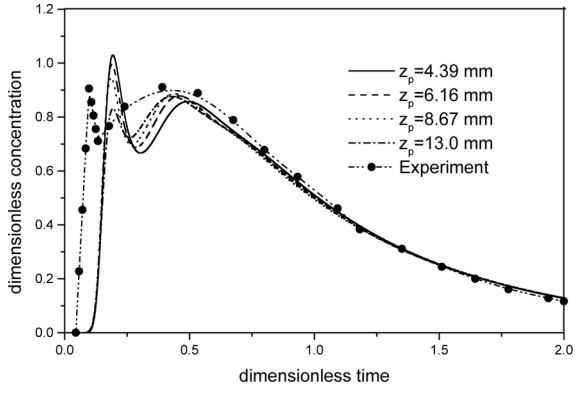


**Figure 3.**
Temporal variation of tracer concentration at the outlet of a single strand tundish: a comparison between experiment and the $k$-$\varepsilon$ turbulence model with different values of $z_p$

| Turbulence models | $t_r$ (s) | $V_p$ | $V_d$ | $V_m$ | $V_m/V_d$ |
|---|---|---|---|---|---|
| Experiment of Singh and Koria, (1987) | 444 | 5.57 | 20.14 | 74.29 | 3.689 |
| $k$-$\varepsilon$ | | | | | |
| $z_p = 4.39$ mm | 444.51 | 10.61 | 20.05 | 69.33 | 3.458 |
| $z_p = 6.16$ mm | 442.2 | 10.43 | 20.46 | 69.11 | 3.378 |
| $z_p = 8.67$ mm | 442 | 10.25 | 20.5 | 69.25 | 3.378 |
| $z_p = 13.0$ mm | 445.7 | 10.25 | 19.84 | 69.91 | 3.523 |
| RNG | 426 | 6.29 | 23.38 | 70.33 | 3.008 |
| CK | 442.5 | 8.63 | 20.4 | 70.97 | 3.479 |
| $k$-$\varepsilon$ with Yap correction | 440.4 | 9.89 | 20.79 | 69.32 | 3.334 |
| LB | 418 | 3.78 | 24.82 | 71.4 | 2.876 |
| CK low Re number model | 481 | 17.08 | 13.49 | 69.43 | 5.147 |
| CK low Re number model with Yap correction | 474.9 | 16.19 | 14.59 | 69.22 | 4.744 |
| Constant effective viscosity model | 488.38 | 8.63 | 12.16 | 79.21 | 6.514 |
| $k$-$\varepsilon$ (SMART) | 441.4 | 14.3 | 20.6 | 65.1 | 3.178 |
| RNG (SMART) | 388 | 6.11 | 30.21 | 63.68 | 2.11 |
| LS | 456 | 8.09 | 17.91 | 74 | 4.132 |

**Table I.**
A comparison of the bulk flow properties obtained from various turbulence models with the experiment

jet impinges on the bottom of the tundish, it spreads in all the direction. But after a while the fluid element going along the $y$ axis meets the wall and will be reflected from the wall towards the center plane. But its reflection or the backward movement will be immediately opposed by the spreading fluid coming from the center of the impingement. So the fluid will not get a chance to go back to the center rather it will be pushed along the wall so that it can move towards the outlet for its discharge. All other fluid packets traveling between an angle of 10 and 90° will hit the wall and similarly will be reflected from the wall but cannot go back to the center again because they will be opposed by the incoming fluid stream and hence they will glide along the wall towards the outlet for their discharge. So the flow will be mostly wall bounded in a region close to the center of impingement and the center line velocity will be less (compared to the velocity at the vicinity of the wall) in this particular case where the side walls are much closer to the point of impingement compared to the outlet. So the concentration of the tracer at the center line is less (away from the center) compared to the wall at the very beginning as predicted by all the four turbulence models (Figures 4 and 9(a)). So it can be seen that the contour of the tracer becomes almost like a "U" or "V" shape (away from the center of impingement) for all the models at the very beginning. Later on there is turbulent mixing of the concentration and the development of the concentration contour is much different for all the models. But at a time of 10 s the concentration contour on the bottom plane has this general feature in all the models when the tracer is just about to spread from its point of impingement.

The use of HOS scheme for the $k$-$\varepsilon$ and the RNG model exactly produced the same concentration contour at the bottom of the tundish at $t = 10$ s, for which

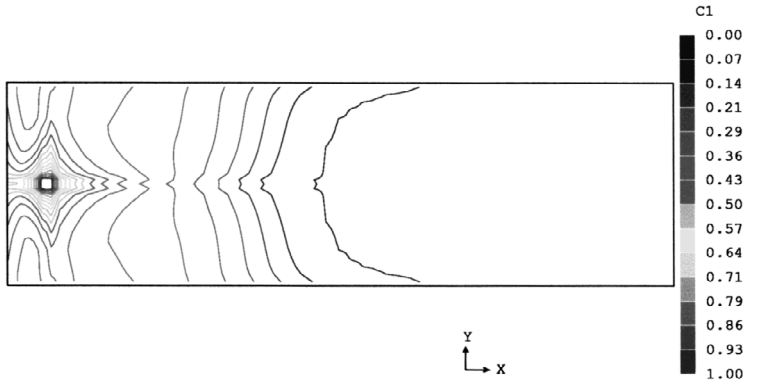


(a)

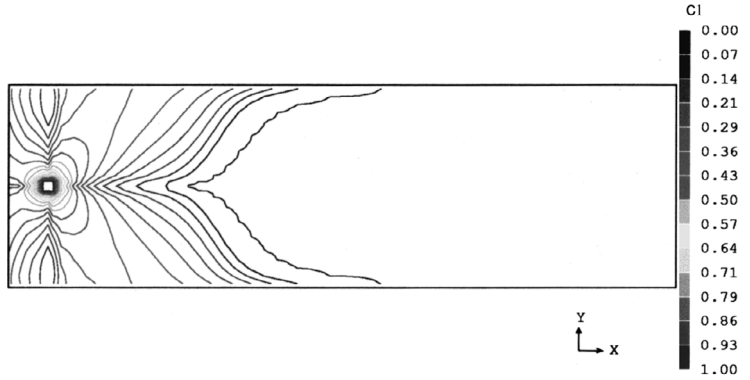


(b)

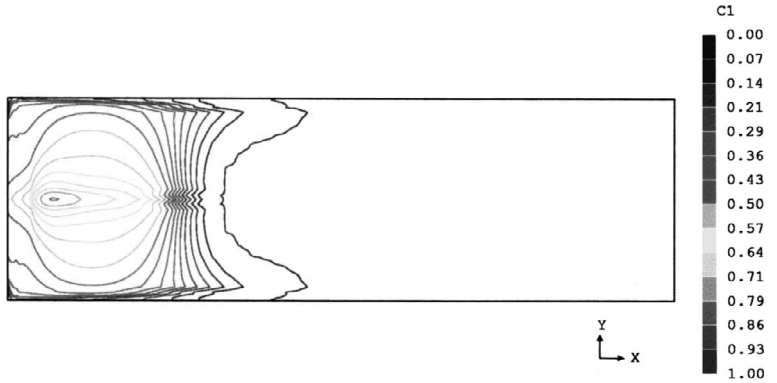


(c)

**Figure 4.**
(a) Concentration isolines at $t = 10$ s for $k$-$\varepsilon$ model, (b) concentration Isolines at $t = 10$ s for RNG model, (c) concentration Isolines at $t = 10$ s for Lam-Bremhorst model

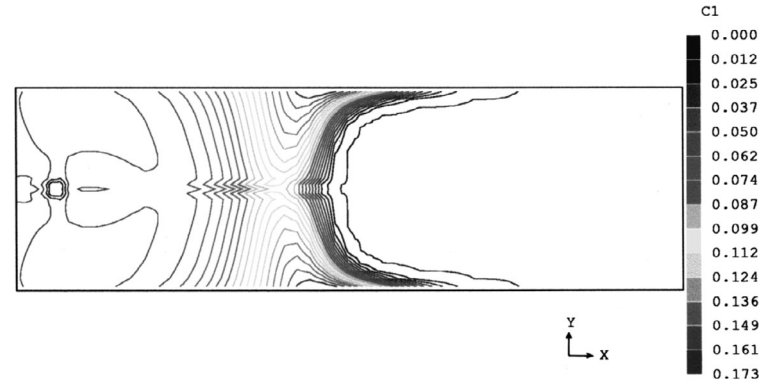


(a)

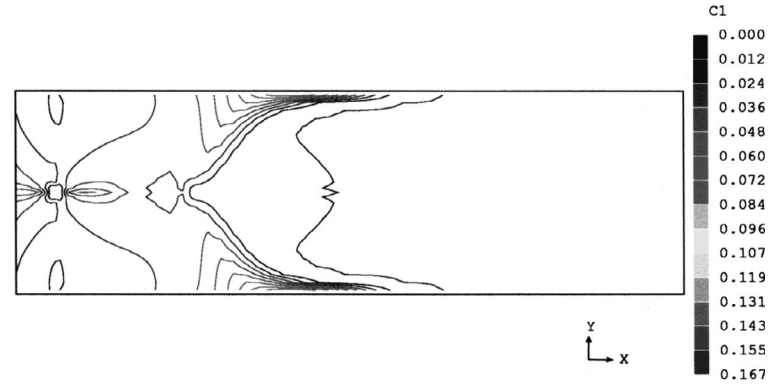


(b)

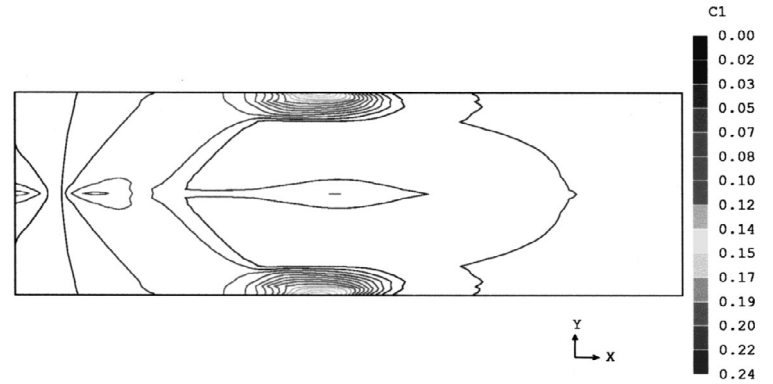


(c)

**Figure 5.**
(a) Concentration Isolines at $t = 20$ s for $k$-$\varepsilon$ model, (b) concentration isolines at $t = 20$ s for RNG model, (c) concentration isolines at $t = 20$ s for Lam-Bremhorst model

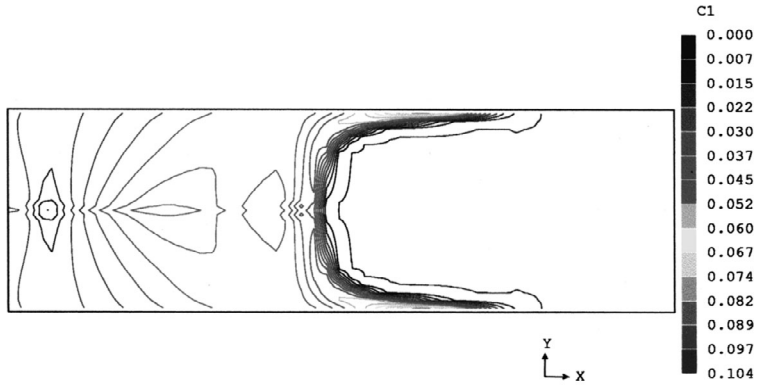


(a)

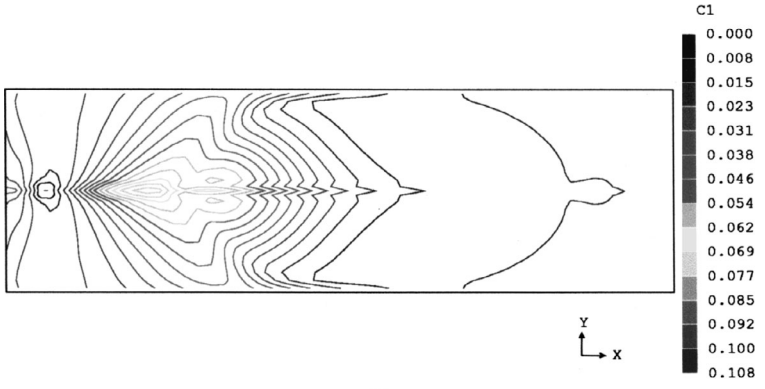


(b)

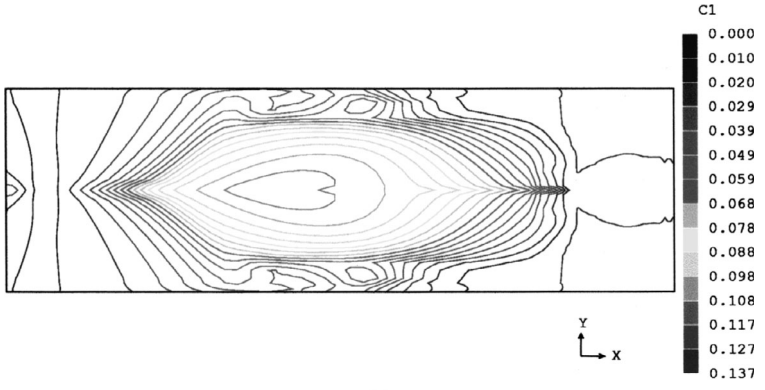


(c)

**Figure 6.**
(a) Concentration isolines at $t = 35$ s for $k$-$\varepsilon$ model, (b) concentration Isolines at $t = 35$ s for RNG model, (c) concentration isolines at $t = 35$ s for Lam-Bremhorst model

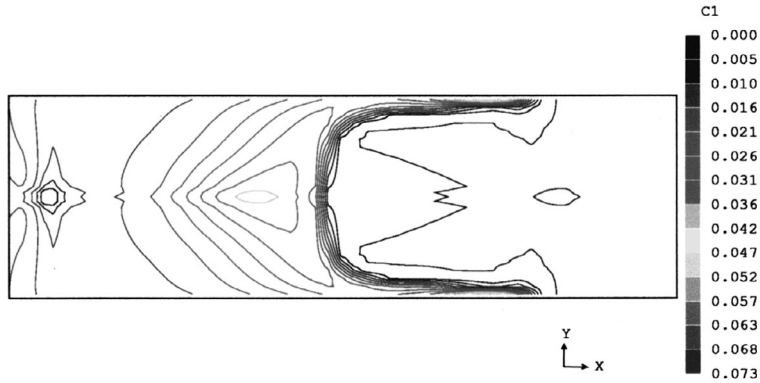


(a)

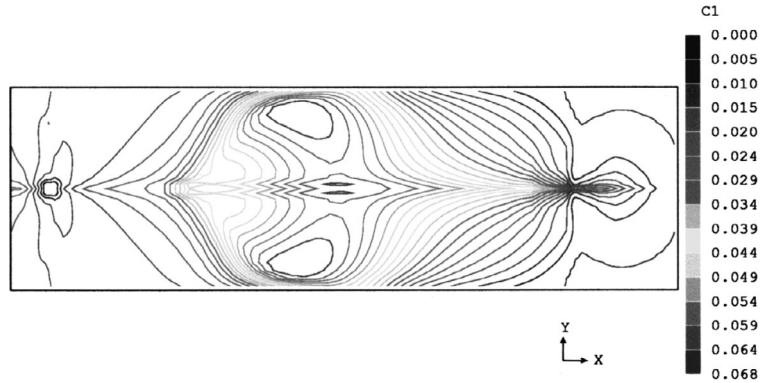


(b)

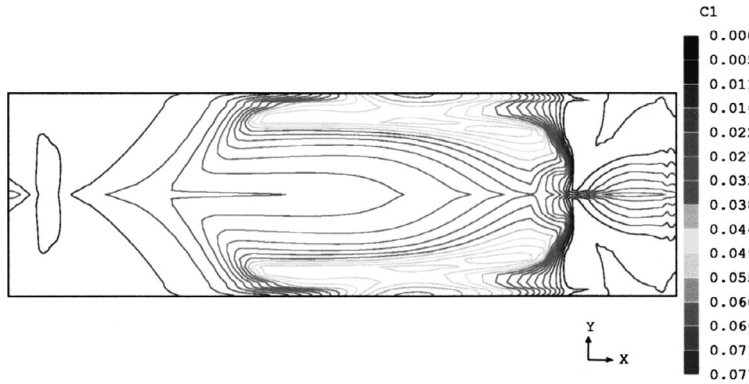


(c)

**Figure 7.**
(a) Concentration isolines at $t = 55$ s for $k$-$\varepsilon$ model, (b) concentration isolines at $t = 55$ s for RNG model, (c) concentration isolines at $t = 55$ s for Lam-Bremhorst model

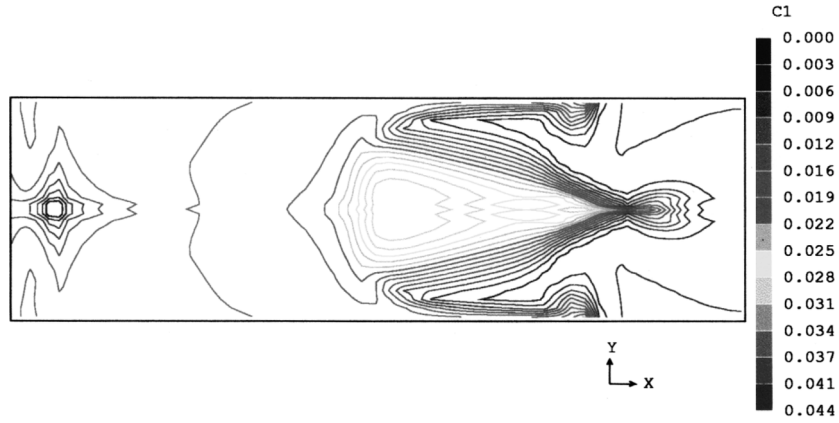


(a)

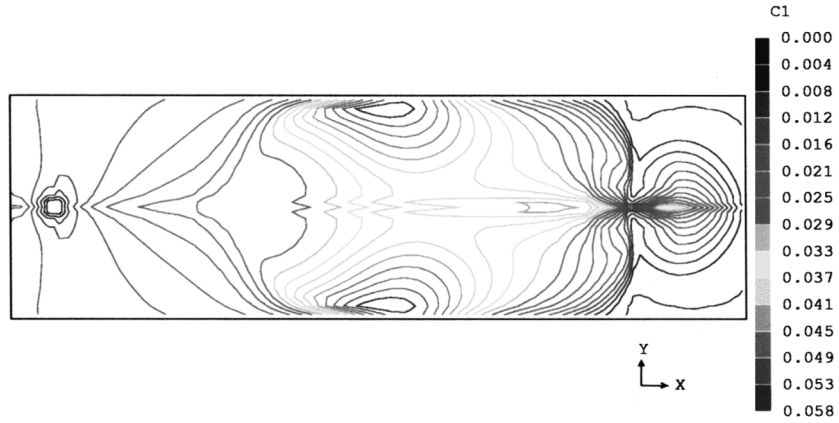


(b)

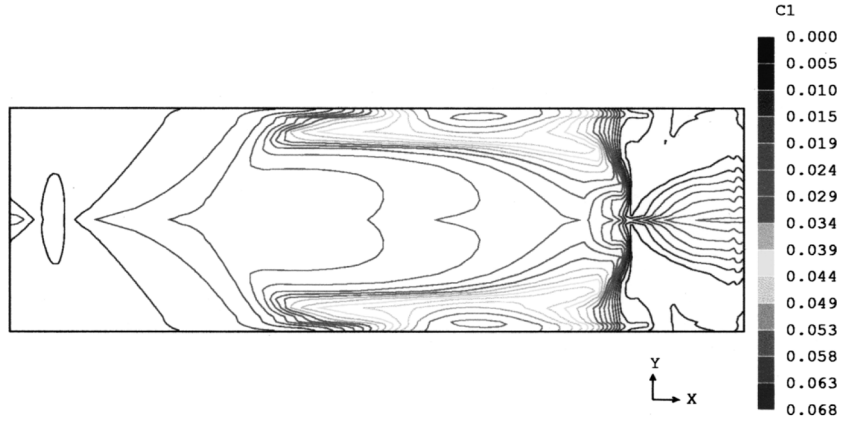


(c)

**Figure 8.**
(a) Concentration isolines at $t = 110$ s for $k$-$\varepsilon$ model, (b) concentration isolines at $t = 65$ s for RNG model, (c) concentration isolines at $t = 60$ s for Lam-Bremhorst model

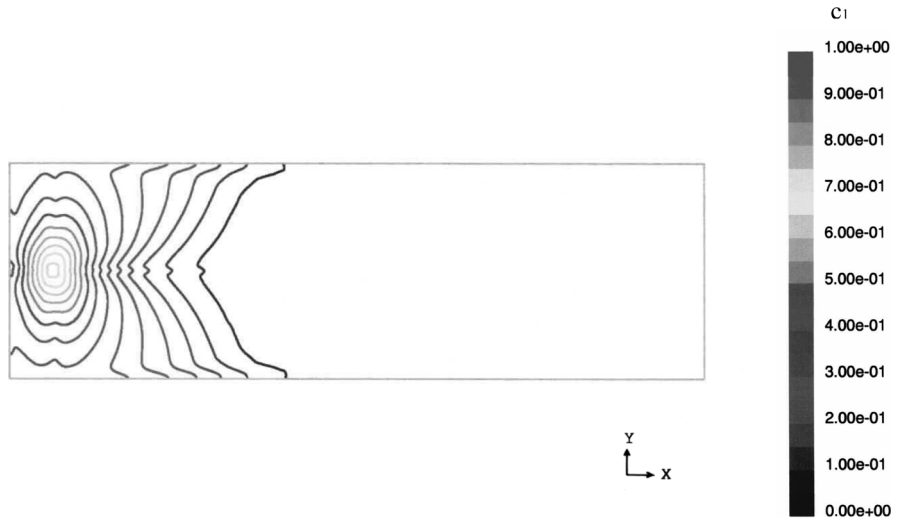


**(a)**

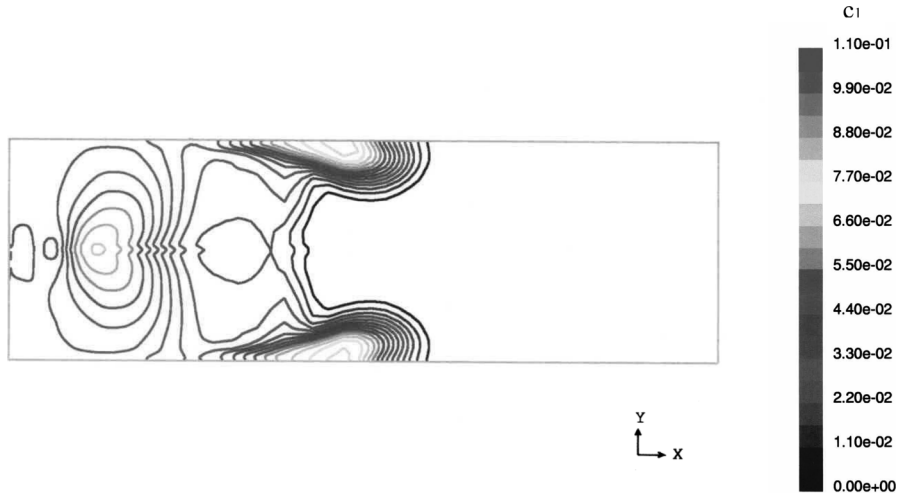


**(b)**

**Figure 9.**
(a) Concentration isolines at $t = 10$ s for LES, (b) concentration isolines at $t = 20$ s for LES, (c) concentration isolines at $t = 35$ s for LES, (d) concentration isolines at $t = 55$ s for LES, (e) concentration isolines at $t = 60$ s for LES, (f) concentration isolines at $t = 70$ s for LES

*(Continued)*

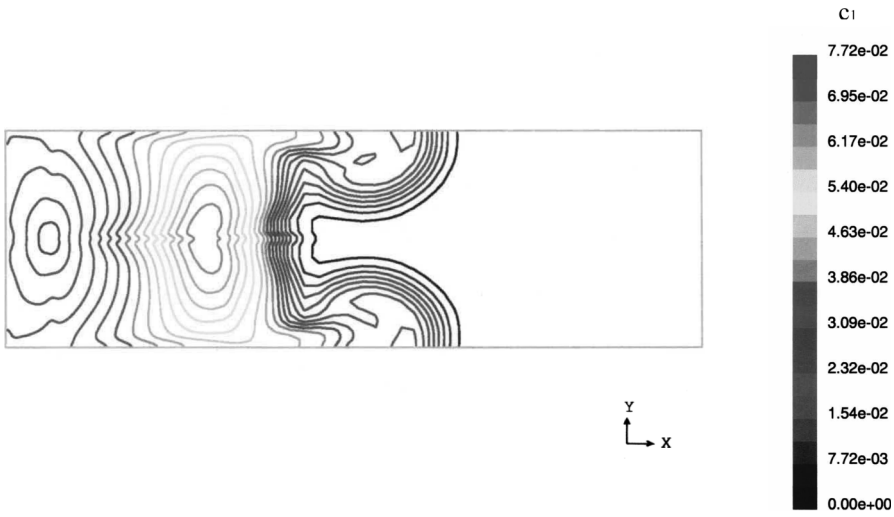


**(c)**

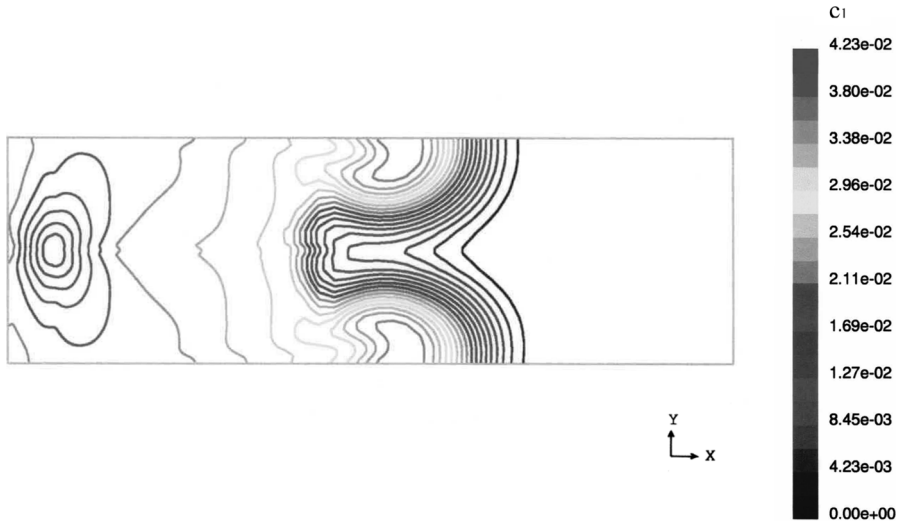


**(d)**

*(Continued)*

**Figure 9.**

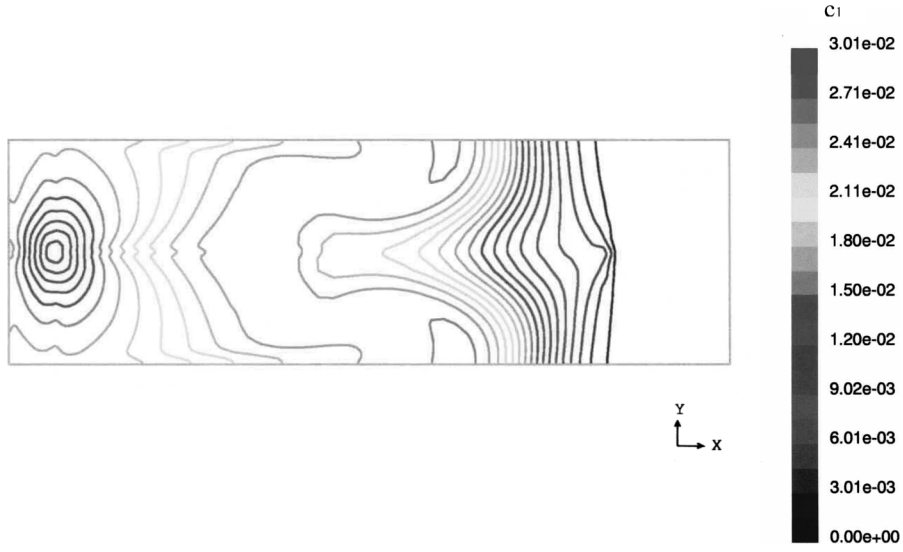
C1
3.01e-02
2.71e-02
2.41e-02
2.11e-02
1.80e-02
1.50e-02
1.20e-02
9.02e-03
6.01e-03
3.01e-03
0.00e+00
Y
X

(e)

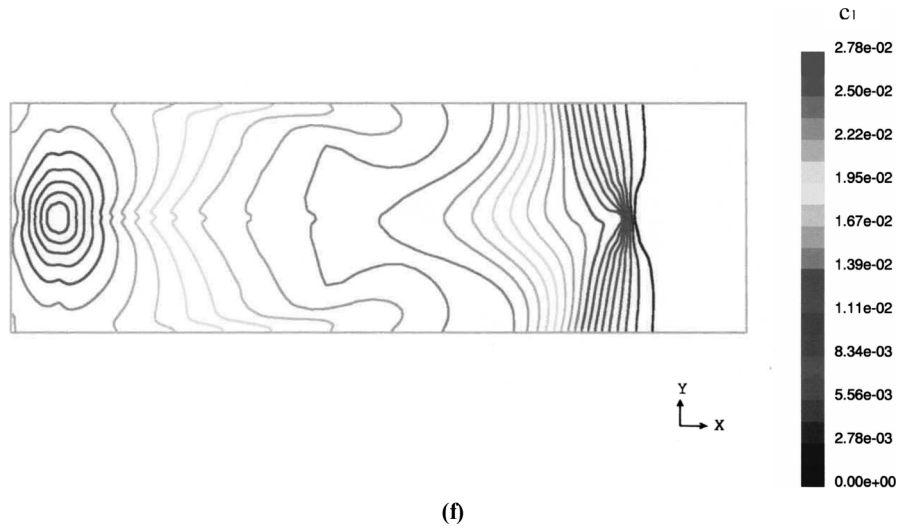
C1
2.78e-02
2.50e-02
2.22e-02
1.95e-02
1.67e-02
1.39e-02
1.11e-02
8.34e-03
5.56e-03
2.78e-03
0.00e+00
Y
X

(f)

**Figure 9.**

they are not repeated here for presentation. After a value of $t > 20$ s, differences could seen in the HOS scheme compared with the hybrid scheme. However, the general pattern of concentration contour looks almost like the hybrid scheme that are shown in Figures 4-8.

At time $t = 20$ s (Figure 5) the tracer has just appeared at the outlet for the LB model while for the $k$-$\varepsilon$ model the concentration away from the outlet is just building on. The $k$-$\varepsilon$ model predicts low value of $k$ near the wall so the wall bounded flow which brings the tracer near to the wall does not allow much of mixing of this tracer with the centerline as a result the tracer proceeds along the wall and the center line concentration evens out due to higher values of turbulent kinetic energy produced in the core of the tundish. But the RNG and the LB model predicts a modest value of $k$ near the wall which allows cross stream mixing of the tracer to some extent so the centre line tracer concentration increases compared to the $k$-$\varepsilon$ model. It can be seen from Figure 5(b) and (c) that the tracer is pushed towards the wall in the RNG and in the LB model and later on with time that diffuses towards the center line.

At a time of 35 s the tracer has appeared at the outlet in the RNG model and for the LB model it is growing at the outlet. It should be marked from the Figure 6(b) and (c) that the outlet is receiving the tracer from the center line at the beginning for these two models. But with the progress of time the tracer which was pushed towards the wall due to a wall bounded flow is slowly diffusing towards the center again and approaching the outlet for its discharge (see Figures 7(b) and 8(b) and (c). Most of the tracer is flowing from the wall towards the center. So the first peak which appeared in the RNG and the LB model is due to the tracer being fed to the outlet via the center line while at a higher time the tracer is fed from the wall for which these two models are capable of showing both the peaks in the tracer concentration.

The wall bounded flow is very much pronounced in the $k$-$\varepsilon$ model and the zone closer to the centerline is having higher $k$ for which the tracer concentration in a zone closer to the centerline is flatter and at the wall the concentration increases with distance along the wall as time progresses. So the contour of tracer concentration (lowest value) looks like a "U" for a longer time (Figures 4(a)-6(a)) after which it converts into a "W" shape due to tracer diffusion from the wall towards the center. The outlet receives the first burst of tracer from the wall at $t = 55$ s (Figure 7(a)). After that the tracer on the center line has reached the outlet and the tracer from the wall is also approaches the outlet due to turbulent diffusion. So the first peak of tracer concentration shown by the $k$-$\varepsilon$ model is due to the tracer coming from the wall and after that the second peak has appeared due to the feeding of the tracer from the center line diffusing from the wall. This is the reason for which the $k$-$\varepsilon$ model could also predict both the peaks in the concentration curve. It must be noticed here that the feeding mechanism of tracer to the outlet is just the opposite compared to the RNG and the LB model.

The LES also is not free from the wall bounded flow for which the tracer concentration at $t = 10$ s looks like a "V" shape, away from the point of impingement. Progressively the tracer gets pushed towards the wall (Figure 9(b)) and the concentration builds near the wall and the center of high concentration moves along the wall (Figure 9(c) at $t = 35$ s). But the tracer gets diffused to the center line in the mid portion of the tundish where convection is much less. This diffusion is mainly due to turbulence. The diffusion of the tracer gets stronger towards the centerline as the outlet is approached. The presence of the outlet in turn makes the local field little stronger which helps the tracer to be convected to the centerline more easily. As a result the centerline concentration increases and the wall concentration falls and the tracer concentration becomes flatter towards the outlet (Figure 9(e) at $t = 60$ s). At the outlet the first burst of tracer appears at $t = 60$ s and the tracer is just centrally fed to the outlet and no other tracer from the wall comes into the outlet because it diffused towards the centerline before it could reach the outlet from the wall. This is the reason why the LES shows only one peak in the tracer concentration curve.

It must be marked that the models which have shown two peaks in the tracer concentration have received the tracer at the outlet in two ways, one from the wall and the other from the center line or just the reverse. But in the LES model there has been stronger diffusional mixing of the tracer prior to its appearance at the outlet for which only one peak is seen and that too the tracer concentration rose much gradually (see Figure 2(c) for comparison) compared to the $k$-$\varepsilon$, the RNG and the LB model. This signifies that the tracer reached the outlet being properly mixed (in the LES simulation) whereas the other three models brought the tracer to the outlet almost unmixed (at the very beginning only) because these models could allow for some plug flow to exist in the tundish. LES, although, created a wall bounded flow near the wall, closer to the point of impingement, but later towards the outlet the flow was properly mixed due to turbulent diffusion for which the tracer could appear at the outlet being thoroughly mixed. The flow could go over a transition from a plug type to a mixed type just before the outlet in the case of a LES simulation. Whereas for the $k$-$\varepsilon$, RNG and the LB the flow continued to remain as plug type near the wall and stretched-up a little further towards the outlet in this manner and the center line flow came as mixed type with some amount of mixing being diffused from the wall towards the center. This is the reason why all these three turbulence models show two types of tracer appearance at the outlet, one being a complete plug type (the initial sudden rise) and the other a mixed type (the second peak and the slow decay of tracer henceforth).

## Conclusions

The mass, momentum and the species conservation equations are solved numerically in a boundary fitted coordinate system comprising a typical

experimental tundish for which experimental measurements of the temporal variation of tracer concentration have been reported. The ratio of the mix to dead volume, and the mean residence time have been analysed from the solution of the species conservation equation and have been compared with nine different turbulence models as well as with the experiment. The analysis of the tracer concentration at the bottom plane of the tundish using the four turbulence models ($k$-$\varepsilon$, RNG, LB and the LES) could demonstrate the presence of plug flow and mixed flow (present in the tundish) and the reason for the two peaks in the tracer concentration and also helped to understand the mechanism of tracer being fed to the outlet.

The standard $k$-$\varepsilon$ high Re number turbulence model, the RNG, the $k$-$\varepsilon$ CK, the $k$-$\varepsilon$ CK with Yap correction and the LES predict the gross flow properties like the mean residence time and the ratio of the mixed to dead volume fairly closely to the accuracy of the experimental measurements while the CK $k$-$\varepsilon$ model predicts the closest value. The LB low Re number model under predicts the mean residence time as well as the ratio of the mixed to dead volume while the other turbulence models over predict these quantities. However, the LB model, compared to all other models, predicts the initial variation of tracer concentration extremely well compared with the experiment.

All the turbulence models (in this study) are able to predict the two peaks in the temporal variation of tracer concentration for a single exit tundish, except the CK Low Re number model, with its Yap correction, the constant effective viscosity model and the LES. It is suggested that the $k$-$\varepsilon$ CK model or the $k$-$\varepsilon$ model can be used for tundish flow to predict overall flow properties because the computation for these models takes less than half the time compared to the LB model or the LES. However, if the prediction of initial transience is of importance due to some reason then the LB low Re number model can be of use.

## References

Chakraborty, S. and Sahai, Y. (1991), "Role of near wall node location on the prediction of melt flow and residence time distribution in tundishes by mathematical modeling", *Metallurgical Transactions*, Vol. 22B, pp. 429-37.

Debroy, T. and Sychterz, J.A. (1985), "Numerical calculation of fluid flow in a continuous casting tundish", *Metallurgical Transactions*, Vol. 16B, pp. 497-504.

Ferziger, J.H. and Peric, M. (1999), *Computational Methods for Fluid Dynamics*, Springer, Berlin, pp. 279-86.

Fluent User's Guide Release 5 (1998), Fluent Inc., Lebanon.

He, Y. and Sahai, Y. (1987), "The effect of tundish wall inclination on the fluid flow and mixing", *Metallurgical Transactions*, Vol. 18B, pp. 81-91.

Illegbusi, O.J. and Szekely, J. (1988), "Fluid flow and tracer dispersion in shallow tundishes", *Steel Research*, Vol. 59, pp. 399-405.

Illegbusi, O.J. and Szekely, J. (1989), "Effect of externally imposed magnetic field on tundish performance", *Ironmaking and Steelmaking*, Vol. 16, pp. 110-5.

Jha, P.K., Dash, S.K. and Kumar, S. (2001), "Fluid flow and mixing in a six-strand billet caster tundish: a parametric study", *ISIJ Int.*, Vol. 41, pp. 1437-46.

Lam, C.K.G. and Bremhorst, K. (1981), "A modified form of the $k$-$\varepsilon$ model for predicting wall turbulence", *Trans ASME Journal of Fluids Engineering*, Vol. 103, pp. 456-60.

Launder, B.E. and Spalding, D.B. (1972), *Mathematical Models of Turbulence*, Academic Press, London.

Levenspiel, O. (1972), *Chemical Reaction Engineering*, Wiley, New York, pp. 253-64.

Lopez-Ramirez, S., Morales, R.D. and Romero Serrano, J.A. (2000), "Numerical simulation of the effects of buoyancy forces and flow control devices on fluid flow and heat transfer phenomena of liquid steel in a tundish", *Numerical Heat Transfer*, Vol. 37A, pp. 69-85.

Madias, J., Martin, D., Ferreyra, M., Villoria, R. and Garamendy, A. (1999), "Design and plant experience using an advanced pouring box to receive and distribute the steel in a six strand tundish", *ISIJ Int.*, Vol. 39, pp. 787-94.

Mazumdar, D. and Guthrie, R.I.L. (1999), "The physical and mathematical modeling of continuous casting tundish systems", *ISIJ Int.*, Vol. 39, pp. 524-47.

Monson, D.J., Seegmiller, H.L., McConnaughey and Chen, Y.S. (1990), "Comparison of Experiment with calculations using curvature – corrected zero and two equations turbulence models for a two-dimensional U-duct", *AIAA*, pp. 90-1484.

Patel, C.V., Rodi, W. and Scheuer, G. (1984), "Turbulence models for near wall and low Reynolds number flows", *AIAA Journal*, Vol. 23, pp. 1308-19.

Phoenics Reference Guide Version 3.2 (1999), CHAM Ltd, London.

Singh, S. and Koria, S.C. (1995), "Study of fluid flow in tundishes due to different types of inlet streams", *Steel Research*, Vol. 66, pp. 294-300.

Singh, S. and Koria, S.C. (1993), "Model study of the dynamics of flow of steel melt in tundish", *ISIJ Int.*, Vol. 33, pp. 1228-37.

Szekely, J. and Themelis, N.J. (1971), *Rate Phenomena in Process Metallurgy*, Wiley, New york, pp. 515-56.

Szekely, J., Illegbusi, O.J. and El-Kaddah, N. (1987), "The mathematical modeling of complex fluid flow phenomena in tundishes", *PhysicoChemical Hydrodynamics*, Vol. 9, pp. 453-72.

Tacke, K.H. and Ludwig, J.C. (1987), "Steel flow and inclusion separation in continuous casting tundishes", *Steel Research*, Vol. 58, pp. 262-70.

Xintian, L., Yaohe, Z., Baolu, S. and Weiming, J. (1992), "Flow behavior and filtration of steel melt in continuous casting tundish", *Ironmaking and Steelmaking*, Vol. 19, pp. 221-5.

Yahkot, Y. and Orszag, S.A. (1992), "Development of turbulence models for shear flows by a double expansion technique", *Phys. Fluids A*, Vol. 4, pp. 1510-20.

Yap, C. (1987), "Turbulent heat and momentum transfer in recirculating and impinging flows", PhD thesis, Faculty of Technology, University of Manchester.

Yeh, J-L., Hwang, W-S. and Chou, C-L. (1992), "Physical modeling validation of computational fluid dynamics code for tundish design", *Ironmaking and Steelmaking*, Vol. 19, pp. 501-4.